A Novel Chassis Concept For Power Steering Systems Driven By Wheel Individual Torque At The Front Axle

M. Sc. Philipp **Kautzmann**
Karlsruhe Institute of Technology, Institute of Vehicle System Technology, Karlsruhe, Germany

M. Sc. Jürgen **Römer**
Schaeffler Technologies AG & Co. KG, Karlsruhe, Germany

Dr.-Ing. Michael **Frey**
Karlsruhe Institute of Technology, Institute of Vehicle System Technology, Karlsruhe, Germany

Dr.-Ing. Marcel Ph. **Mayer**
Schaeffler Technologies AG & Co. KG, Karlsruhe, Germany

Summary

The project "Intelligent Assisted Steering System with Optimum Energy Efficiency for Electric Vehicles (e²-Lenk)" focuses on a novel assisted steering concept for electric vehicles. We analysed different suspensions to use with this innovative power steering concept driven by wheel individual drive torque at the front axle. Our investigations show the potential even for conventional suspensions but reveal the limitations of standard chassis design. Optimized suspension parameters are needed to generate steering torque efficiently. Requirements arise from emergency braking, electronic stability control systems and the potential of the suspension for the use with our steering system. In lever arm design a trade-off between disturbing and utilizable forces occurs. We present a new design space for a novel chassis layout and discuss a first suspension design proposal with inboard motors, a small scrub radius and a big disturbance force lever arm.

1 Introduction

Electric vehicles are a promising opportunity to reduce local greenhouse gas emissions in transport and increase overall energy efficiency, as electric drivetrain vehicles operate more efficiently compared to conventionally motorized vehicles. The internal combustion engine of common vehicles not only accelerates the vehicle, but also supplies energy to on-board auxiliary systems, such as power-assisted steering, which reduces the driver’s effort at the steering wheel. In electric vehicles, this energy is provided by battery, reducing the vehicle’s range. Considering new features offered by the drivetrain of electric cars, this issue may be solved.

Wheel individual drive torque at the front axle influences the steering torque. To benefit from this feature, we design a suitable chassis concept as well as an intelligent torque control. The development of this chassis concept with focus on the front suspension is part of our research project e²-Lenk. This research collaboration between Karlsruhe Institute of Technology (KIT) and Schaeffler Technologies AG & Co. KG, deals with an energy-efficient assisted steering system by using intelligent torque control of individual wheel drives. The project was launched in January 2015 and is subsidized by the Federal Ministry for Education and Research (BMBF).

As mentioned before our goal is to use wheel individual drives at the front axle to reduce the driver´s effort at the steering wheel. Fig. 1 shows the front axle of a car driving in a left curve. Lateral forces $F_{S,l/r}$ induce a self-aligning torque around the steering axis EG. This results in a torque M_H at the steering wheel, which the driver has to counteract.

To reduce the steering wheel torque, our power steering system applies a higher longitudinal force to the outer wheel (in this case on the right side). The disturbance force lever arms r_{AN} transfers the longitudinal forces and induces a torque on the steering axis. The generated torque reduces the self-aligning torque and the steering wheel torque.

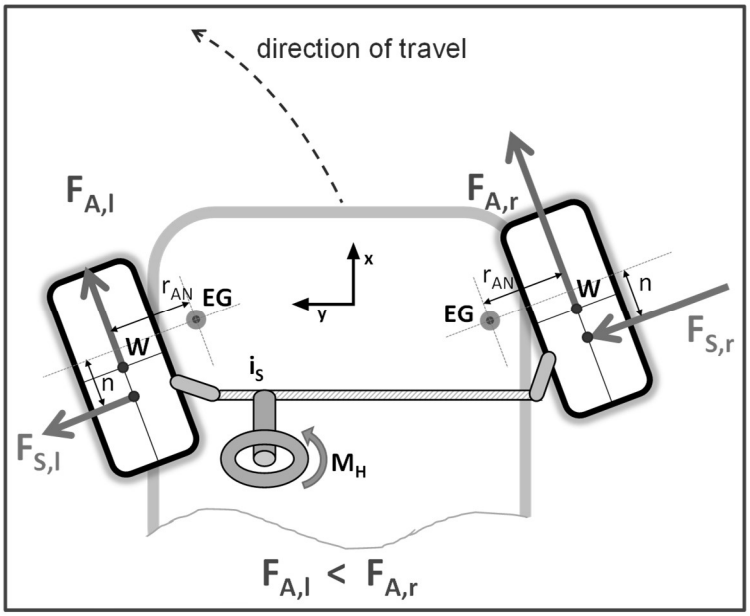

M_H	Steering wheel torque
n	Caster trail
r_{AN}	Disturbance force lever arm
$F_{S,l/r}$	Lateral forces
$F_{A,l/r}$	Longitudinal forces
W	Tire contact patch
EG	Steering axis
i_s	Steering ratio

Fig. 1: Principle of a power steering system driven by wheel individual torque

2 Theoretical Background

2.1 State of research

During our research we found publications dealing with wheel individual drive torque and influences on the steering wheel torque. Torque vectoring at the front axle can improve driving dynamics but may cause disturbing steering forces [2]. Hence chassis concepts like "RevoKnuckle" try to reduce the disturbance forces to the steering system by shortening the disturbance force lever arm [1]. But there are benefits of wheel individual torque at the front wheels. Skid steering is a method to steer around a corner without a steering angle at the wheels. The system generates slip angles at the wheels as a result of a yaw moment around the vertical vehicle axis caused by drive torque distribution [9]. We found methods to influence the steering wheel torque by wheel individual breaking. In this case the generated steering torque is proportional to the scrub radius [3].

Li-Qiang Jin et al. investigated a concept called driving power steering (DFPS) producing steering torque using motorized wheels and a suspension with a positive scrub radius. Their system is able to reduce the steering wheel torque while driving and standing still [4]. Kristof Polmans et al. show the feasibility of a steering system steered by wheel individual drive torque. During their investigations they also detected a reduced maximum lateral acceleration because of additional longitudinal forces in the tire contact zone. They mention the different disturbance force lever arms. However, they use a concept car with wheel hub motors [5]. J. Wang et al. investigated a vehicle with a scrub radius of 70 mm and wheel hub motors. They reduced the steering wheel torque significantly by wheel individual torque control. Their system is named DDAS. Feng-Kuang Wu et al. investigated a car with a scrub radius of 240 mm and wheel hub motors. They are able to reduce the steering wheel torque to zero by wheel individual torque control, but recommend a traction control to drive on slippery road [6].

The research projects above show the potential of the steering system, but also point out some problems. All systems use wheel hub motors. In this case acceleration and deceleration forces affect the same lever arm in the suspension. However, we could not find investigations of vehicle concepts using inboard motors transmitting torque by drive shafts. This changes the effective lever arm as described in chapter 2.2. There are no simulations with a complex multibody car simulation model to analyse the new steering system at the car´s limits. We also could not find analyses about influences of different tire characteristics, especially the variable length of the pneumatic trail.

2.2 Suspension parameters and influences on the steering wheel torque

Fig. 2 shows the most important suspension parameters for a steering system powered by wheel individual drives.

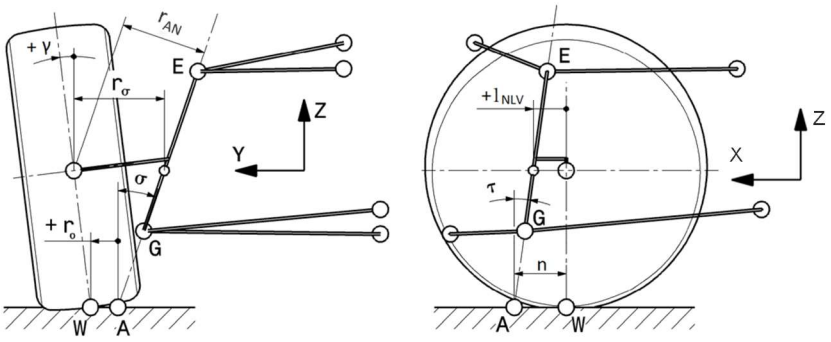

Fig. 2: Suspension parameter [7]

The horizontal distance projected on the YZ plane, between the intersection of the kingpin axis and the ground, to the centre of the contact patch is called scrub radius r_0. The scrub radius of conventional suspensions is in a range between -20 mm and 65 mm [8]. It affects the lever arms transmitting longitudinal and vertical tire force to a torque around the steering axis. The caster offset at the ground n transfers lateral force from cornering as a torque on the steering axis. For cars with a power steering system it is in a range between 20 mm and 60 mm [8]. As a self-aligning torque is required by law (ECE R 79), the design space for the caster trail is limited. The additional influences of the pneumatic trail need to be considered.

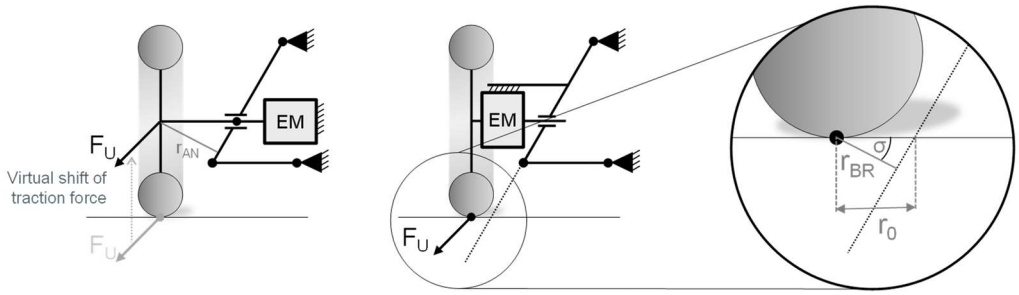

Fig. 3: Difference between the relevant disturbance force lever arms of powertrains with in board motors (r_{AN}) and wheel hub motors (r_{BR})

Depending on the powertrain concept the two different lever arms transfer longitudinal forces and induce a steering torque on the steering axis. The acceleration disturbance force lever arm r_{AN} shown in Fig. 3 transfers longitudinal acceleration forces generated by inboard motors as a torque on the steering axis. For in wheel motors the braking disturbance force lever arm r_{BR} is the relevant length. It is defined as the product of scrub radius and the cosines of caster and kingpin angles [7]. In conventional suspensions the lever arm r_{AN} is bigger than r_{BR}.

The wheel load lever arm transfers vertical tire force as a torque on the steering axis. It is influenced by the kingpin inclination angle σ, the caster angle τ as well as the caster offset at the ground n and the scrub radius r_0 [7].

2.3 Influences of tire characteristics

The pneumatic trail describes the longitudinal distance from the centre of the contact patch to the centroid of all lateral forces applied to the contact patch during cornering. It is defined as positive when the centroid is located after the centre of the contact patch. The pneumatic trail has a high impact on the self-aligning torque, which significantly affects the steering wheel torque [7]. High side slip angle can cause a reduced or negative pneumatic trail, resulting in a lower or negative self-aligning torque. A reduced self-aligning torque reduces the required longitudinal force in the tire contact patch using our steering system. As shown in Fig. 4 the self-aligning torque decreases before the maximum lateral force is reached [10]. A power steering system driven by wheel individual torque can benefit from this phenomenon, because reduced drive torque distribution is needed to support the driver at the car´s limit.

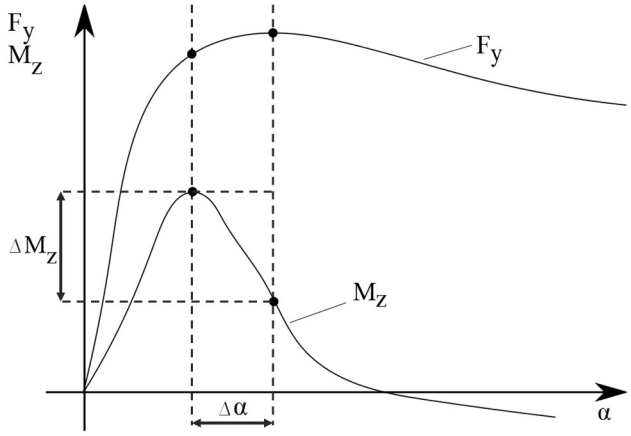

Fig. 4: Self-aligning torque M_z and lateral force F_Y for a tire vs slip angle α. The self-aligning torque decreases (ΔM_Z) before the maximum lateral force is reached (according to [10])

Fig. 5 shows the friction circle for pure lateral force and with combined forces. The peak lateral force of the tire is dependent on the longitudinal force. If the steering system needs a high longitudinal force to reduce the steering torque the peak lateral acceleration will decrease significantly. Hence, the longitudinal force needs to be minimized.

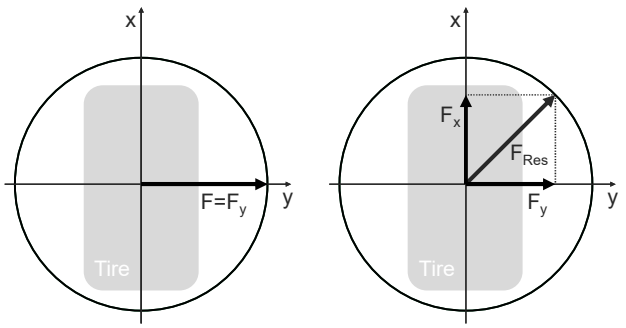

Fig. 5: Influences of the friction circle on a steering system driven by wheel individual drive torque

3 Method

To gain knowledge about the feasibility of a power steering system driven by wheel individual torque at the front axle, simulations using CarMaker® are conducted. The vehicle model is based on the standard vehicle (DemoCar) modified with an electric, wheel individual drive at the front axle. Our goal is to investigate different chassis designs and their influences on the steering wheel torque. Therefore we used IPG Kinematics ™ to generate suspensions within and out of the usual range. The tested suspensions are designed with similar steering kinematics and cause a similar restoring torque. We choose three driving manoeuvres to show the comparability between the four suspensions, including the potential of steering wheel torque reduction and the influences of disturbance forces.

The vehicle is divided into mechanical and non-mechanical subsystems such as suspension, steering system, drive system, tires or control units. This allows to use components with different degrees of detail as it is necessary for individual analysing purposes. Therefore multibody simulation models are suitable tools for designing system components, control and assistance systems, for analysing energy demands and for reviews regarding driving comfort. For analyses below we use IPG CarMaker® as simulation software, which offers a multibody simulation model for overall vehicle simulation.

3.1 Vehicle Model

IPG CarMaker® is delivered with a combustion engine driven standard vehicle (DemoCar) representing a compact car. Because we analyse the influence of wheel-individual driving torques relative to the driver's steering wheel torque, we use an electric car based on CarMaker's standard vehicle Fig. 6.

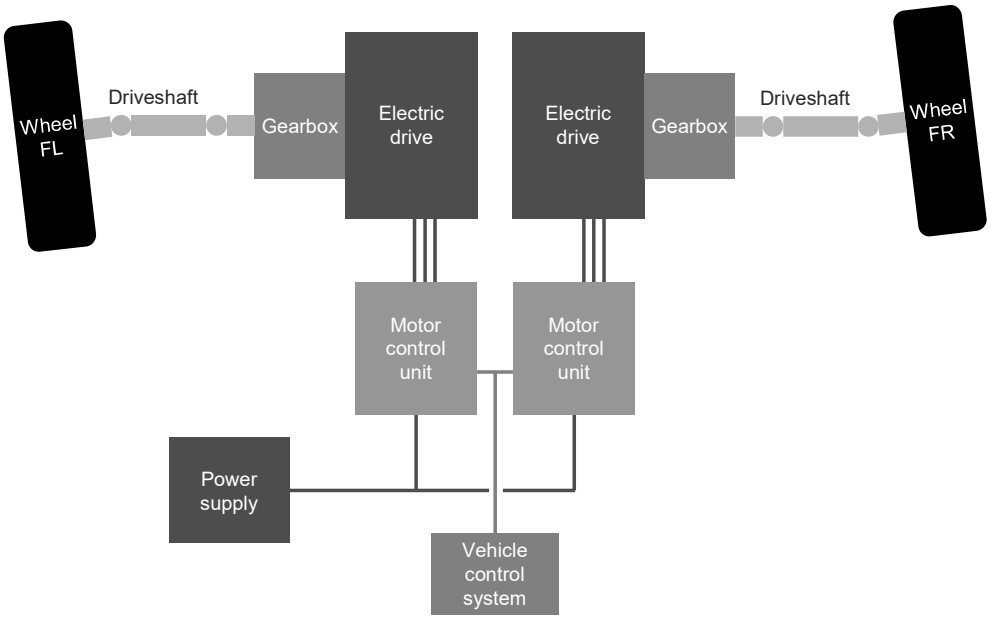

Fig. 6: Vehicle Model - Front axle and driveline with wheel individual electric inboard motors, gearbox and driveshaft

In contrast to the standard variant, we substitute the combustion engine with two inboard electric drives at the steered front axle. This powertrain is based on the performance data of an electric middle class vehicle. We use IPG´s RealTime Tire (195 65 R15), as it is able to handle combined longitudinal and lateral tire forces. Furthermore we implement different suspension modifications as described in chapter 4.3.

Component	Data
Vehicle Mass	1463 kg
Wheelbase	2.53 m
Track Width	1.51 m
Tires	195 65 R 15
Electric Drives Mechanical Power Maximum Torque Maximum rot. Speed Average Efficiency Gear Ratio	two inboard drives 65 kW (each) 125 Nm (each) 10500 rpm (each) 95 % i = 9
Suspension	Double wishbone (4 different variations)

Tab. 1: Vehicle data

3.2 Tested front suspensions

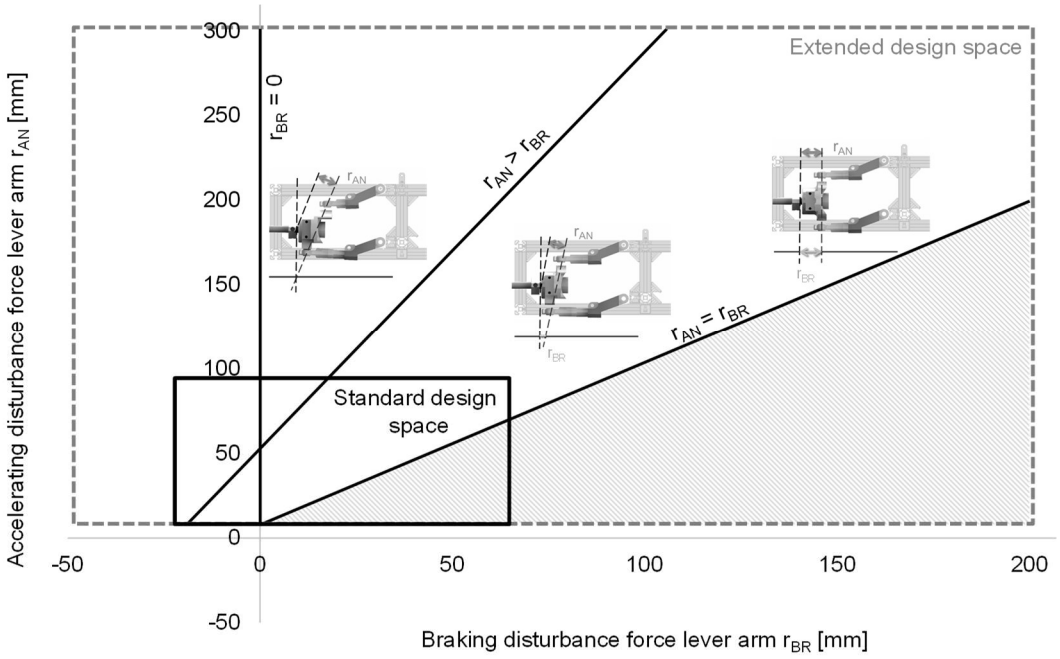

Fig. 7: Design space of the disturbance force lever arms influencing a power steering system driven by wheel individual torque at the front axle. The values of the standard design space are based on information of Heißing [8].

The main suspension parameters influencing the steering system driven by wheel individual drive torque are r_{AN} and r_{BR}. The standard design space of these parameters is shown in Fig. 7. To test the novel steering system we also want to consider suspensions in the extended design space. Hence we design 4 different front suspensions for the vehicle model. All suspensions are designed as double wishbones. The caster trail of our suspensions is 20 mm. The main difference between these suspensions are kingpin angles and scrub radius.

Parameter		Suspension 1	Suspension 2	Suspension 3	Suspension 4
Scrub radius [mm]	r_0	0	0	70	0
Disturbance force lever arm (braking) [mm]	r_{BR}	0	0	68	0
Kingpin offset at hub level [mm]	r_σ	70	0	140	140
Disturbance force lever arm (accelerating) [mm]	r_{AN}	68,2	0	136,4	129,3
Kingpin inclination angle [°]	σ	13	0	13	22,5
Wheel load lever arm [mm]	p	4,5	0	14,5	8,5
Caster trail [mm]	n	20	20	20	20

Tab. 2: Suspension parameters of tested front suspensions

The suspension parameters of suspension 1 are very similar to those of the standard DemoCar. We expect some influence on the steering torque caused by torque distribution at the front axle but no effect while braking. We design suspension 2 with a scrub radius and a disturbance force lever arm of zero. We expect no influence on the steering torque while braking or accelerating. Suspension 3 and 4 have a big disturbance force lever arm. For both suspensions we expect explicit influence on the steering torque caused by torque distribution at the front axle. Suspension 3 has a scrub radius of 70 mm. Hence, we expect a high influence of braking forces on the steering system. Suspension 4 has a scrub radius of zero but a very big kingpin inclination angle. We expect a high influence on the steering torque caused by torque distribution at the front axle but no effect while braking.

3.3 Driving manoeuvres

To test our chassis concepts we simulate three different driving manoeuvres. With the first manoeuvre we show the comparability between the self-aligning torques of the tested front suspensions. We use manoeuvre 2 to show the potential of steering wheel torque reduction. In manoeuvre 3 we analyse the influences of disturbance forces on the steering system.

3.3.1 Manoeuvre 1: Slowly accelerated circle with equally distributed drive torque at the front wheels

In this driving manoeuvre the car drives in a circle with a constant radius of 100 m. The coefficient of friction is 1.0. The car starts in the middle of the road at a speed of 0 km/h. At the beginning the steering wheel is in neutral position. The car is accelerated with a low acceleration of 0.1 m/s² to reduce influences of acceleration resistance. The driver pilots the car in the middle of the road. To stop the simulation at peak lateral acceleration we detect the steering wheel acceleration exceeding 0.5 rad/s², above which point the driver is struggling to maintain a steady state circle (steering acceleration becomes inconsistent). For suspension 1 the peak lateral acceleration is 8.25 m/s². Therefore, we end all simulations at this lateral acceleration. The powertrain provides an equal drive torque at each of the front wheels. Fig. 8 shows the steering wheel torque vs the lateral acceleration of our car with suspension 1 driving this manoeuvre. This behaviour is very similar to the standard IPG DemoCar. Therefore, we use this chart as reference to compare our suspensions.

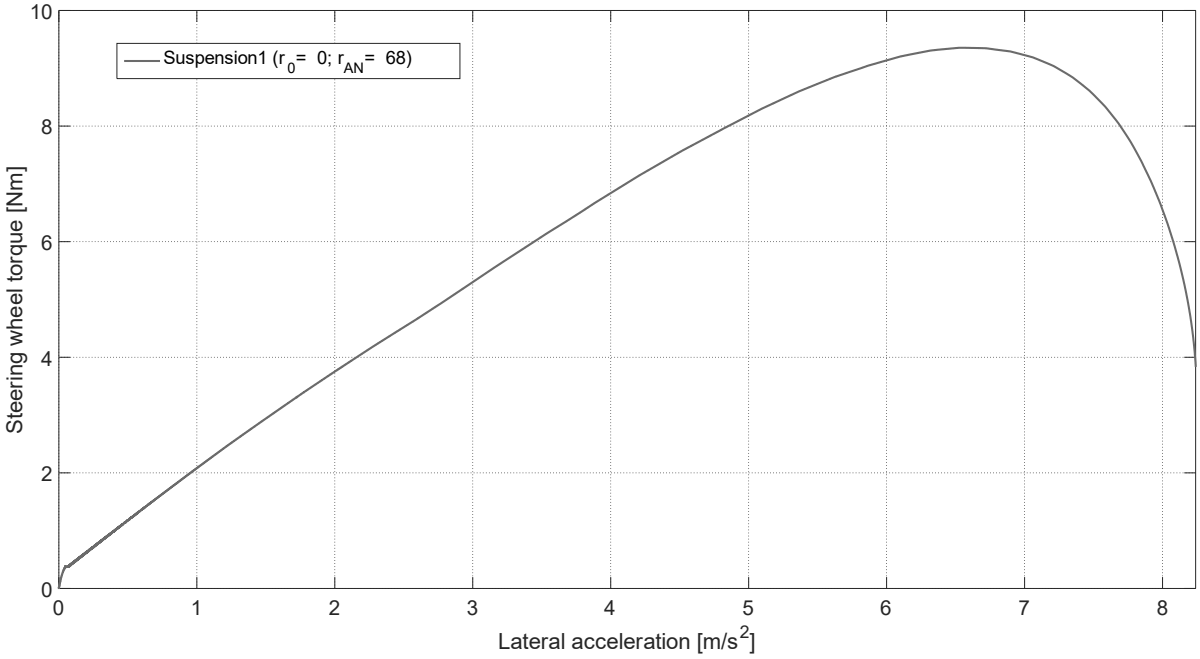

Fig. 8: Steering wheel torque vs lateral acceleration for suspension 1 while driving the slowly accelerated Circle with equally distributed drive torque at the front wheels

3.3.2 Manoeuvre 2: Slowly accelerated circle with drive torque distribution at the front wheels (principle of e²-Lenk)

This driving manoeuvre is equal to the one in chapter 3.3.1 but a torque distribution is applied to the front wheels. To focus on influences of the suspension and to avoid influences of the control system we use a simplified torque distribution control between left and right wheel. Linear dependent on the steering wheel torque the motor control unit adds a drive torque to the outer wheel and subtracts a drive torque of the inner wheel. Fig. 9 shows the drive torques for manoeuvre 1 and manoeuvre 2 with suspension 1 implemented.

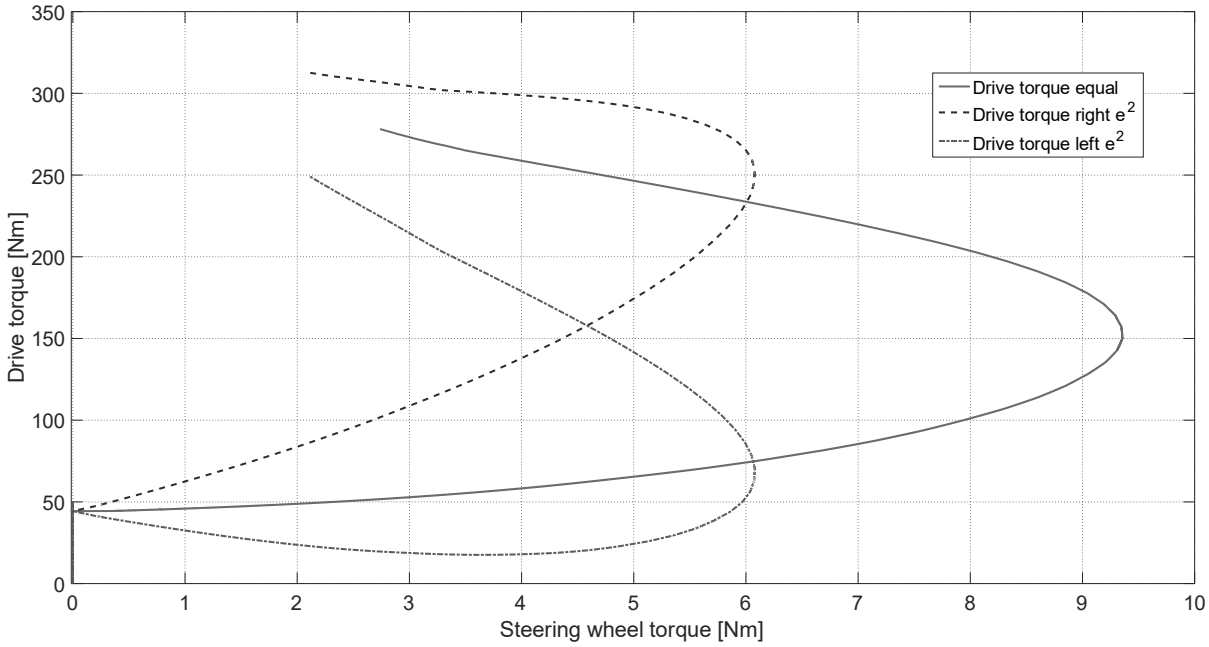

Fig. 9: Drive torques vs steering wheel torque for torque distribution at the front axle (e²) compared to equally distributed drive torque

3.3.3 Manoeuvre 3: Straight-ahead accelerating and braking on surfaces with split coefficient of friction

To gain information about the influence of disturbing forces, we test the behaviour of the car while accelerating and braking on surfaces with split coefficient of friction. The car is controlled by the IPG driver model. The car drives in a straight, 10 meters wide road. The right side has a low coefficient of friction μ (μ=0.1), the left side has a normal coefficient of friction (μ=1). The driver pilots the car on the middle of the road and accelerates to 100 km/h with less than 1 m/s². After 40 seconds, the driver brakes with a maximum deceleration of 2.3 m/s². We choose low acceleration rates because a driver would not accelerate fast on surfaces with split coefficient of friction but he will apply the highest controllable deceleration rate to simulate emergency braking.

4 Simulation results

In the following we present the results of our investigations. We simulate the three manoeuvres each with the car model and our four suspensions presented in chapter 3.2.

4.1 Manoeuvre 1: Slowly accelerated circle with equally distributed drive torque at the front wheels

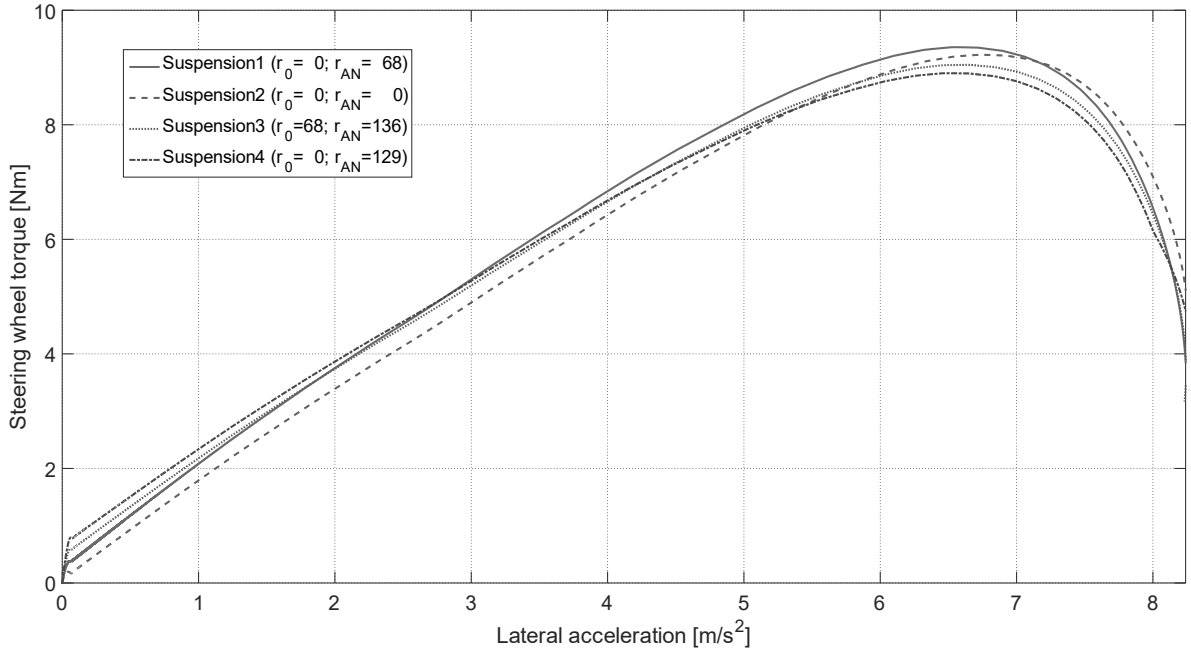

Fig. 10: Steering wheel torque vs lateral acceleration for a slowly accelerated circle with equally distributed drive torque at the front wheels. The steering wheel torque for the different suspensions shows similar behaviour.

Fig. 10 shows the steering wheel torque of the tested suspensions as a function of lateral acceleration while driving the slowly accelerated circle with equal drive torque at the front wheels. It becomes apparent that all four suspensions cause a similar steering wheel torque. At low speed the steering wheel torque differs because of the influences of the wheel load lever arm. The car starts with a speed and a steering wheel angle of zero. To set the right steering angle for cornering, the required steering wheel torque depends on the suspension. Higher lateral accelerations increase the steering wheel torque until a lateral acceleration of approximately 7 m/s² is reached. As mentioned in chapter 2.3 the pneumatic trail has significant influence on the steering wheel torque. This is the reason for the phenomenon of the steering wheel torque decreasing around 50% (5 Nm) for lateral accelerations higher than 7 m/s².

4.2 Manoeuvre 2: Slowly accelerated circle with drive torque distribution at the front wheels (principle of e²-Lenk)

Based on the circle test manoeuvre with torque distribution at the front axle we observed two effects. The torque vectoring effect due to the torque distribution at the front wheels and an influence of the steering wheel torque for all suspensions except suspension 1. As shown in Fig. 11 the steering wheel torque depends on the suspension design. The results show that it is possible to reduce the steering wheel torque more than 50% using a steering system powered by wheel individual torque at the front axle. Applying the e²-Lenk torque distribution, there is no reduction of the maximum lateral acceleration. We reach maximum lateral acceleration of 8.25 m/s² with all tested suspensions.

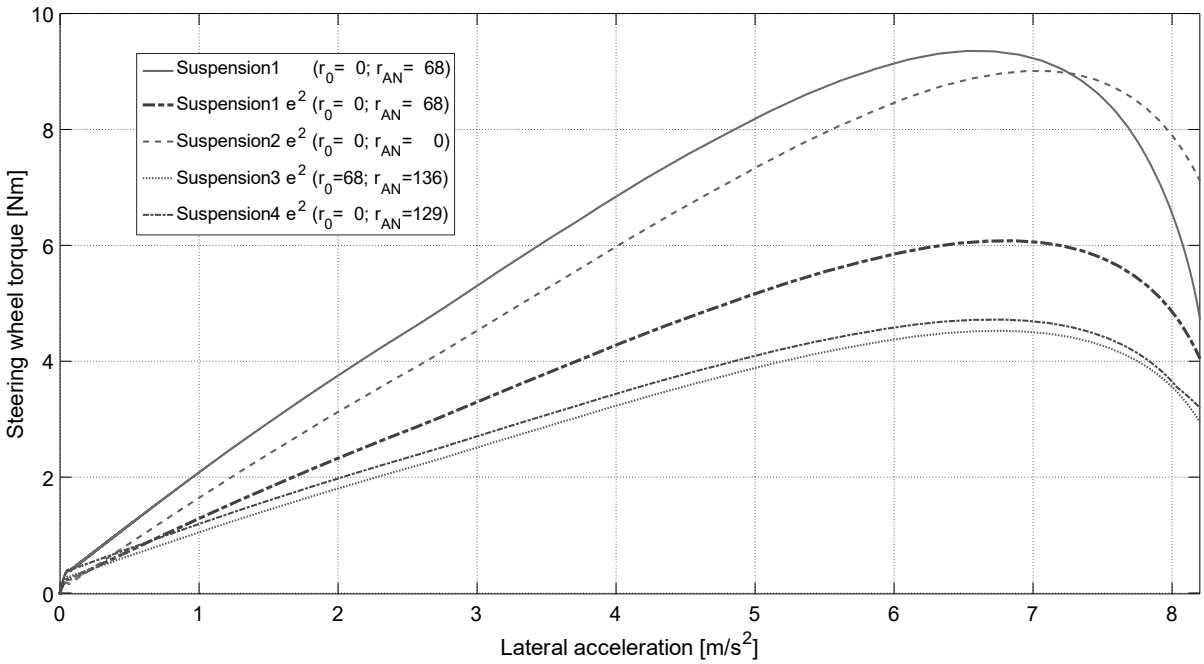

Fig. 11: Steering wheel torque vs lateral acceleration for the four suspensions with torque distribution (e²) compared to the reference (suspension 1 with equally distributed drive torque at the front axle). The steering wheel torque is highly dependent on the suspension design.

4.3 Manoeuvre 3: Straight-ahead accelerating and braking on surfaces with split coefficient of friction

The figure below shows the resulting steering wheel torque in manoeuvre 3. Fast acceleration on surfaces with split coefficient of friction causes a torque difference at the drive wheels, because the wheel on the side with a higher coefficient of friction is able to transfer a higher force. The high influences of the disturbance force lever arm while accelerating is shown in Fig. 12. As expected, suspension 3 generates the highest steering wheel torque, because of the biggest disturbance force lever arm. The driver decelerates the car after 40 s. Suspensions 1, 2 and 4 show a different behaviour in the decelerating manoeuvre. We didn´t expect that, because all suspensions have the same influence on the steering wheel torque with respect to lateral acceleration. We assume the wheel load lever arm as the reason for this effect in dynamic manoeuvre. As the lever arm of vertical force correlates to the cosines of the kingpin inclination angle, braking on surfaces with split coefficient of friction causes a yaw moment. The driver needs to control the car to compensate this moment. This changes the balance of wheel load to the outer wheel and causes steering torque because of the wheel load lever arm. With suspension 3 implemented, the driver requires a high steering wheel torque above 20 Nm which is hardly controllable for a driver.

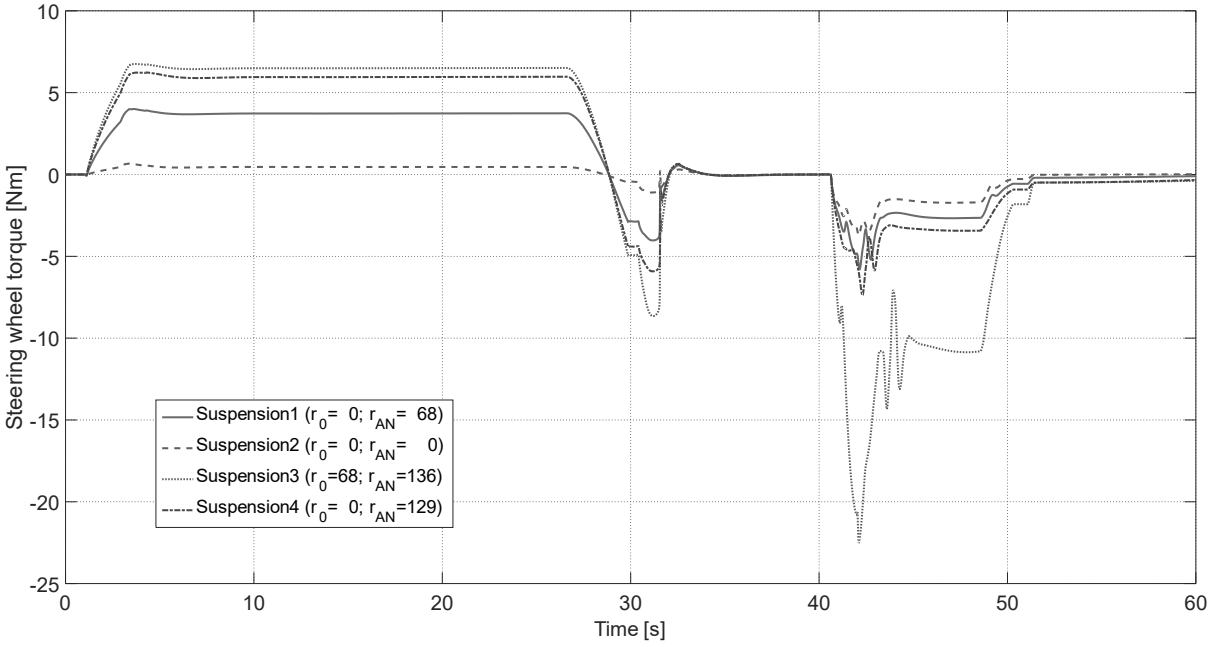

Fig. 12: Straight-ahead accelerating and braking on surfaces with split coefficient of friction.

5 Conclusion

Using a car with wheel individual electric inboard drives, we compared different suspensions for the use with a power steering system driven by wheel individual torque at the front axle.

Without the drive torque distribution, the steering wheel torque of the vehicle is similar for all tested suspensions while driving on a slowly accelerated circle. Our investigation shows the influence of the pneumatic trail on the self-aligning torque. For high acceleration rates the self-aligning torque decreases up to 50%. The wheel load lever arm highly influences the steering wheel torque at low speed. By adding a drive torque distribution, the steering wheel torque differs between the test runs depending on the tested suspension. We show the potential of steering torque reduction, which correlates to the length of the disturbance force lever arm. Our investigation proves the potential of our steering system also for high acceleration rates. Driving on surfaces with split coefficient of friction leads to two characteristics. A long disturbance force lever arm causes a big steering wheel torque while accelerating. This can be solved by an intelligent vehicle control system but a reduced longitudinal acceleration. A long scrub radius causes a steering wheel torque while braking. Reducing the maximum deceleration is not acceptable for safety reasons. This leads to the requirement of a small scrub radius.

In our investigation we also detected a reduced power consumption in a wide range of driving situations. Details are documented in "Energetic analysis of wheel-individual torque variation as EPS-substitution for electric vehicles" [11].

Our investigations show the feasibility of a steering system powered by wheel individual drive torque at the front axle. To validate our data a real 1:1.5 scale model is in production. The novel chassis concept is powered by inboard motors. Simulations show the best results for suspensions are those with suspension parameters outside the standard design space. The front suspension needs a small scrub radius, a short wheel load lever arm and a big disturbance force lever arm. These suspension parameters can´t be changed independently. Additionally, influences to driving dynamics, torque vectoring and disturbance forces need to be considered which lead to new boundary conditions. Therefore, an optimization process is needed.

6 Acknowledgement

This work has been supported by the Federal Ministry for Education and Research (BMBF) in the project "Intelligent Assisted Steering System with Optimum Energy Efficiency for Electric Vehicles (e²-Lenk)" under grant FKZ 16EMO0073K, 16EMO0074.

7 References

[1] Frantzen, M.; Simon, M.; David, W.; Ohra-aho, L.
Reduktion Störender Lenkmomente
Springer Fachmedien ATZ 05/2004, pp. 434 - 440
Wiesbaden, 2004

[2] Höck, M.; Auweiler, M.; Nett, H.; Hoffmann, W.
Drehmomentverteilung im Frontantrieb
Springer Fachmedien ATZ 06/2009, pp. 446 - 453
Wiesbaden, 2009

[3] Dominguez-Garcia, A.; Kassakian, J.; Schindall, J.
A backup system for automotive steer-by-wire, actuated by selective braking
IEEE 35th Annual Power Electronics Specialists Conference
Aachen, 2004

[4] Li-Qiang, J.; Song, C.; Hu, C.
Driving Force Power Steering for the Electric Vehicles with Motorized Wheels
IEEE Vehicle Power and Propulsion Conference, pp. 1518-1524
Dearborn, 2009

[5] Polmans, K.; Stracke, S.
Torque vectoring as redundant steering for automated driving or steer-by-wire
Springer Fachmedien, P.E. Pfeffer (Ed.), 5th International Munich Chassis Symposium 2014, Proceedings, DOI 10.1007/978-3-658-05978-1_13
Wiesbaden, 2014

[6] Wu, F.; Yeh, T.; Huang, C.
Motor control and torque coordination of an electric vehicle actuated by two in-wheel motors
Elsevier Ltd., Mechatronics
Oxford, 2012

[7] Harrer, M.; Pfeffer, P.
Lenkungshandbuch
Springer Vieweg
Wiesbaden, 2013

[8] Heißing, B.; Ersoy, M.; Gies, S.
Fahrwerkhandbuch (4. Auflage)
Springer Vieweg
Wiesbaden, 2013

[9] Gao, S.; Cheung, N.; Cheng, E.
Skid Steering in 4-Wheel-Drive Electric Vehicle
IEEE, 7th International Conference on Power Electronics and Drive Systems
Bangkok, 2007

[10] Unrau, H.; Frey, M.; Fertig, M.
Grundsatzuntersuchung zum quantitativen Einfluß von Reifenbauform und -ausführung auf die Fahrstabilität von Kraftfahrzeugen bei extremen Fahrmanövern
FAT Schriftreihe 192
Frankfurt a. M., 2005

[11] Römer, J.; Kautzmann P.; Mayer, M. Ph.; Frey, M.
Energetic analysis of wheel-individual torque variation as EPS-substitution for electric vehicles
Tag des Fahrwerks 2016
Aachen, 2016